

Supplementary information for

**“A trigonal prismatic mononuclear cobalt(II) complex showing  
single-molecule magnet behavior”**

by Valentin V. Novikov\*, Alexander A. Pavlov, Yulia V. Nelyubina,

Marie-Emmanuelle Boulon, Oleg A. Varzatskii,

Yan Z. Voloshin, Richard E.P. Winpenny\*

**This file includes:**

Supplementary Methods

Supplementary Figures S1 to S5

Supplementary Tables S1 to S4

Supplementary References

## Supplementary methods

### *Magnetic measurements*

Magnetic measurements have been performed using a MPMS SQUID magnetometer from Quantum Design. Finely ground microcrystalline powder of **2** was immobilized in eicosane matrix inside a polycarbonate capsule. Both the contributions of the eicosane and the capsule have been subtracted from the data obtained.

### *NMR spectroscopy*

<sup>1</sup>H and <sup>13</sup>C NMR spectra were recorded from dichloromethane-d<sub>2</sub> solutions of the complex **2** using a Bruker Avance 600 FT-spectrometer (600.22 and 150.94 MHz, respectively).

Paramagnetic shifts in the NMR spectra were calculated as a difference between chemical shifts of the nuclei of the paramagnetic cobalt(II) complex **2** and those of its isostructural diamagnetic zinc-containing analogue<sup>43</sup>. Contact Fermi contributions to the paramagnetic shifts were estimated by DFT calculations (see below). The remaining part of the paramagnetic shifts had the dipolar origin and depended on polar coordinates of the corresponding nuclei in the coordinate frame of the unpaired electron:

$$\delta_{pcs} = \frac{1}{12\pi r^3} \Delta\chi_{ax} (3\cos^2\theta - 1) \quad (S1)$$

where  $\Delta\chi_{ax}$  – an axial anisotropy of the magnetic susceptibility tensor, m<sup>-3</sup> and  $r$  and  $\theta$  – polar coordinates of a nucleus in the magnetic susceptibility tensor frame. Given relative remoteness of most nuclei of apical substituents from the paramagnetic ion, a point-dipole approximation was employed. A possible rhombicity of the magnetic susceptibility tensor was not taken into account owing to  $C_3$ -symmetry of the complex **2**. The value of  $\Delta\chi_{ax}$  was estimated by fitting the experimental pseudocontact shifts to those calculated by Eq. 1 using the experimental molecular geometry. Fitting of the temperature dependence of the NMR-derived anisotropy of the magnetic susceptibility was performed using the Van-Vleck formulae for a high-spin d<sup>7</sup> ion<sup>44</sup>:

$$\Delta\chi_{ax}(T) = \chi_{\parallel}(T) - \chi_{\perp}(T) = \frac{\mu_B g_{\parallel}^2}{4kT} \cdot \frac{1+9e^{-2D/kT}}{1+e^{-2D/kT}} - \frac{\mu_B g_{\perp}^2}{kT} \cdot \frac{1+\frac{3kT}{4D} \cdot (1-e^{-2D/kT})}{1+e^{-2D/kT}} \quad (S2)$$

where  $D$  — axial zero field splitting energy,  $g_{\parallel}$  and  $g_{\perp}$  — parallel and perpendicular components of g-tensor, respectively,  $\mu_B$  — Bohr magneton,  $kT$  — thermal energy.

### *Quantum chemical calculations*

All quantum chemical calculations were performed with ORCA package v. 3.0.3<sup>45</sup>. X-ray data were used as an initial structure for geometry optimization performed with a non-hybrid PBE functional,<sup>46</sup> the scalar relativistic zero-order regular approximation (ZORA)<sup>47</sup> and the scalar relativistically recontracted (SARC)<sup>48</sup> version of the def2-TZVP basis set<sup>49</sup>. No significant difference in the calculated magnetic parameters was found if the experimental X-ray geometry with optimized positions of hydrogen atoms was used instead of a fully optimized structure.

For calculation of the NMR paramagnetic shifts, the solvation effects were taken into account using the COSMO model.<sup>50</sup> Fermi coupling constants were calculated using a hybrid PBE0 functional<sup>51</sup> and a basis sets def2-TZVP modified by addition of the primitives with a higher order of exponent to improve the description of the electron density close to a nucleus (the corresponding values of the Gaussian primitive were equal to 68.16 and 16371.074 for hydrogen and second period elements (C, F), respectively). Contact shifts were calculated using the following equation:<sup>52</sup>:

$$\delta_{FC} = \frac{S(S+1)\mu_B}{3kTg_N\mu_N} \cdot \bar{g} \cdot A_{iso} \quad (S3)$$

where  $A_{iso}$  — isotropic hyperfine coupling constant,  $\bar{g}$  — rotationally averaged electronic g-value,  $g_N$  — nuclear g-value,  $\mu_B$  and  $\mu_N$  — Bohr and nuclear magnetons, respectively,  $kT$  — thermal energy.

#### *Calculation of magnetic properties using program PHI*

The observed temperature-dependence of magnetic susceptibility curves were fitted in Phi software by spin Hamiltonian:

$$\hat{H} = \frac{D}{3} \hat{O}_2^0 + E \hat{O}_2^2 + \mu_B g B \hat{S} \quad (S4)$$

where  $\hat{O}_2^0$  and  $\hat{O}_2^2$  are Stevens operators:

$$\hat{O}_2^0 = 3L_z^2 - L^2 \quad (S5)$$

$$\hat{O}_2^2 = \frac{1}{2} (L_+^2 - L_-^2) \quad (S6)$$

No separate terms for orbital contribution were employed. Although the values of g—tensor obtained demonstrated very slight rhombicity ( $g_{yy} = 2.12$ ,  $g_{xx} = 2.20$ ), we limited its symmetry to axial ( $g_{\parallel} = g_{zz}$ ,  $g_{\perp} = (g_{xx} + g_{yy})/2$ ) to simplify the comparison with data from other methods.

*Ab initio* CASSCF calculations were performed using def2-TZVPP basis set for cobalt and def2-TZVP<sup>49</sup> for all other atoms of **2**, together with the corresponding auxiliary basis sets, starting from the natural orbitals from a tightly converged restricted open shell Hartree-Fock calculation. The active space for CASSCF calculations was chosen to consist of five cobalt d-based molecular orbitals occupied by seven electrons (CAS(7, 5)) with 10 quadruplet and 40 doublet electronic states taken into account. To speed up the calculations, the ‘chain-of-spheres’ (RIJCOSX) approximation to exact exchange as implemented in ORCA was applied. To account for dynamic correlations, N-electron valence perturbation theory (NEVPT2) calculations were performed on top of CASSCF-converged wave functions. To obtain ZFS parameters, the effect of spin-orbit coupling are treated using multireference internally contracted configuration interaction (MRCI) module of Orca software.

#### *Calculation of magnetic properties from CASSCF/NEVTP2*

Magnetic properties were calculated within the approach from<sup>53</sup>. Magnetization and magnetic susceptibility may be calculated as follows:

$$M_a = -\frac{\partial E_a}{\partial B_a} \quad (S7)$$

$$\chi_{ab} = \frac{\partial M_a}{\partial B_b} \quad (S8)$$

where  $a, b = x, y, z$ .

Molar magnetization is a sum of the magnetization of each state weighted by its Boltzmann population:

$$M_a = \frac{\sum_{i=1}^N \frac{\partial E_i}{\partial B_a} e^{\frac{-E_i}{kT}}}{\mu_B \sum_{i=1}^N e^{\frac{-E_i}{kT}}} = \frac{kT}{\mu_B} \frac{\partial \ln Z}{\partial B_a} \quad (S9)$$

where  $Z$ —a partition function equal to  $\sum_{i=1}^N e^{\frac{-E_i}{kT}}$ .

The values of  $\chi$ -tensor elements are expressed as follows:

$$\chi_{ab} = \frac{\partial M_a}{\partial B_b} = \frac{N_A kT}{10} \frac{\partial^2 \ln Z}{\partial B_a \partial B_b} \quad (S10)$$

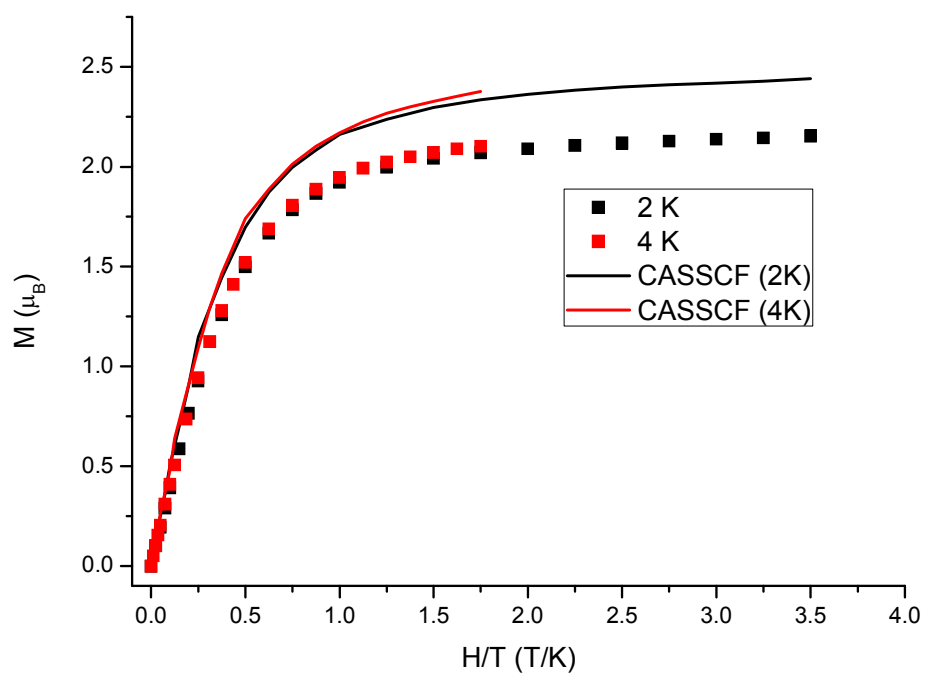
Anisotropic components of the magnetization and the magnetic susceptibility were calculated from the energy levels of **2** in an external magnetic field  $B$  ranging from 0 to 7 T with a step 0.05 T; those were obtained from CASSCF/NEVTP2/MRCI calculations. Isotropic values of the magnetization and the magnetic susceptibility were calculated by the following equations:

$$M_{iso} = \frac{M_x + M_y + M_z}{3} \quad (S11)$$

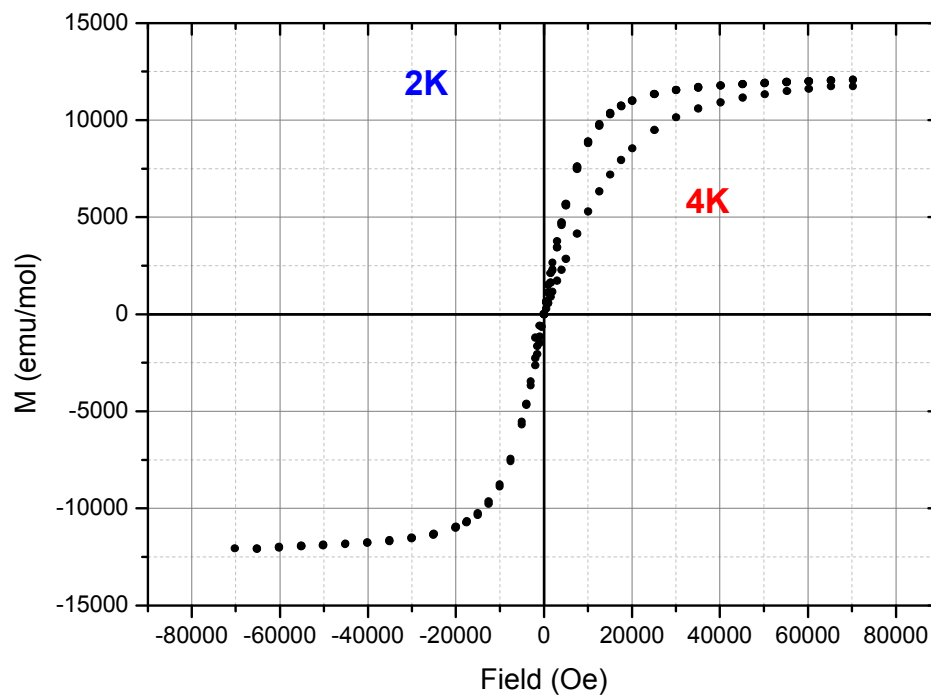
$$\chi_{iso} = \frac{\chi_{xx} + \chi_{yy} + \chi_{zz}}{3} \quad (S12)$$

The value of anisotropy of the magnetic susceptibility tensor was calculated as follows:

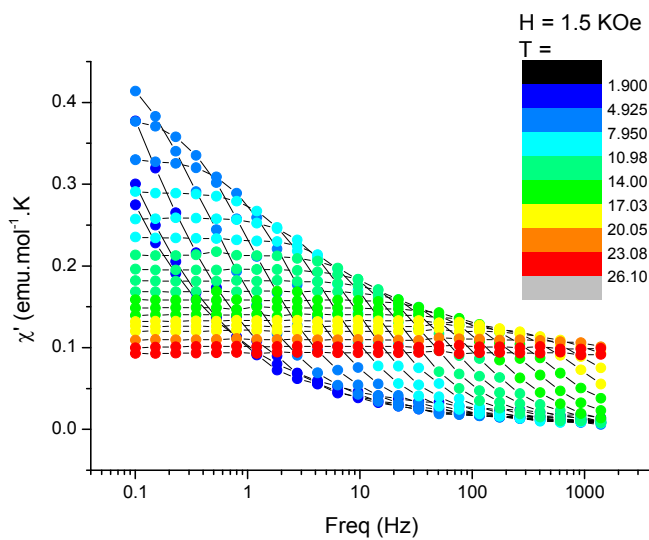
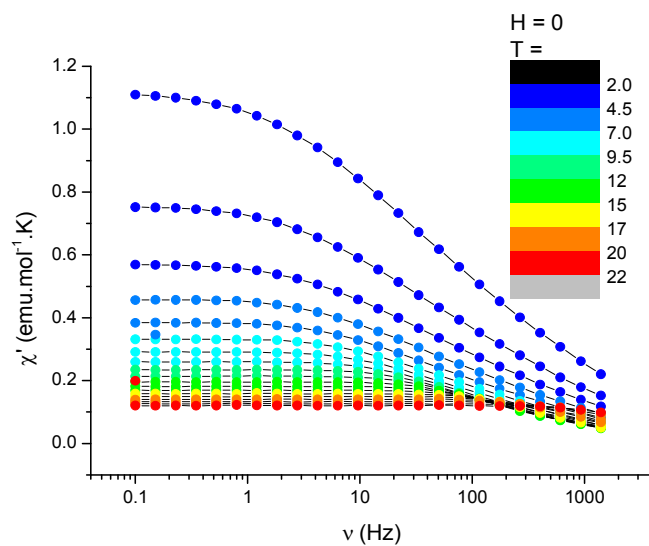
$$\Delta\chi_{ax} = \chi_{zz} - \frac{\chi_{yy} + \chi_{xx}}{2} \quad (S13)$$



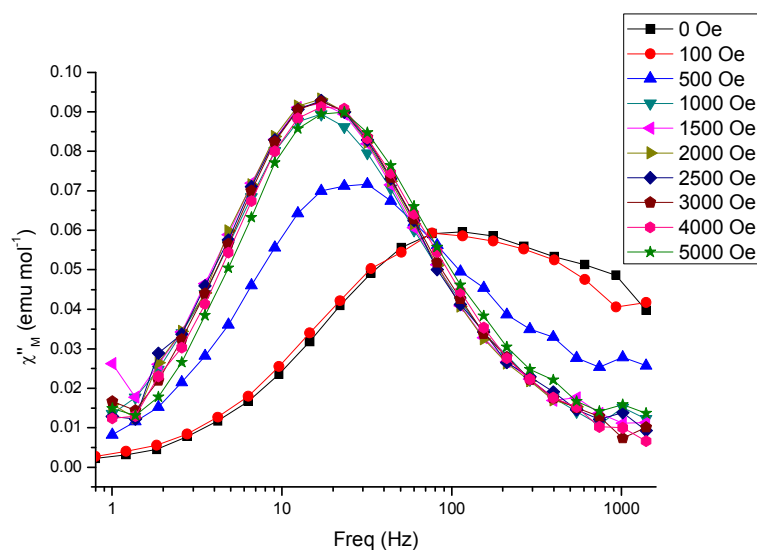
**Supplementary Figure S1.** Variable-field magnetization data for **2** collected at 2 and 4 K and their CASSCF-based simulations.



**Supplementary Figure S2.** Variable-field magnetization data for **2** collected at 2 and 4 K. Data were obtained by starting at  $T = 2\text{ K}$ ,  $H = 0\text{ T}$ , sweeping to  $H = -7\text{ T}$  and then sweeping to  $+7\text{ T}$ . Then temperature was changed to 4 K and field was sweep back to  $H = 0\text{ T}$ .

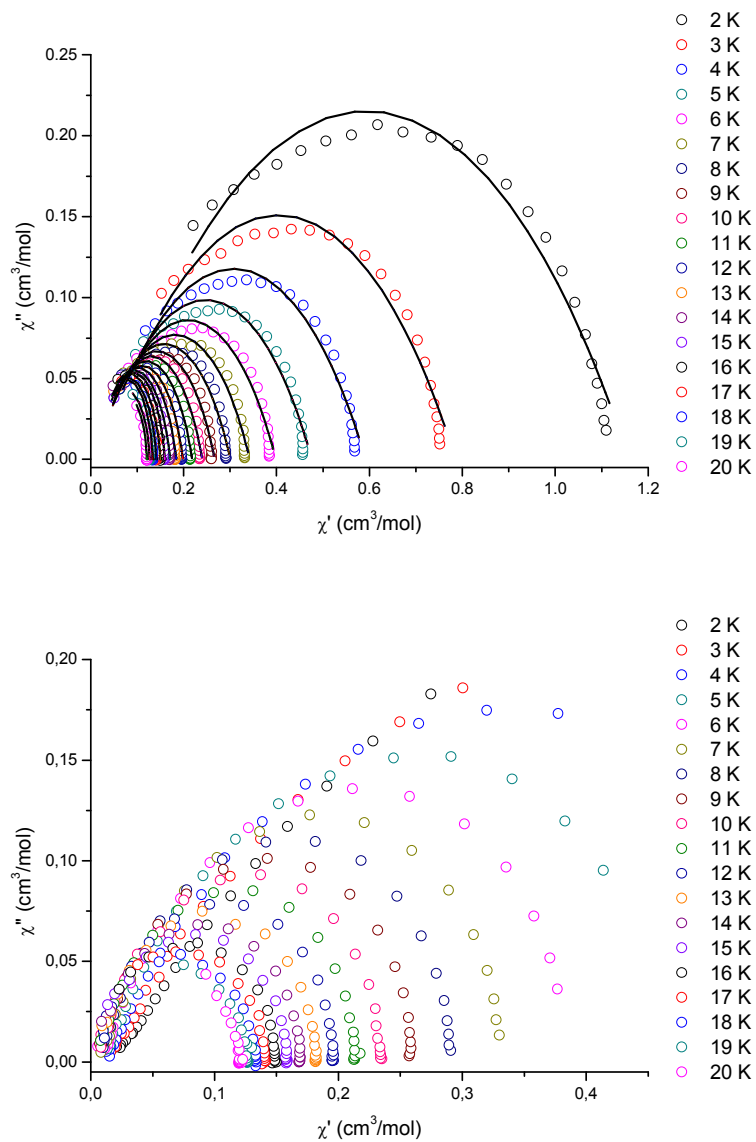


**Supplementary Figure S3.** Variable-temperature, variable-frequency in-phase  $\chi'_M$  components of the a.c. magnetic susceptibility collected for a microcrystalline sample of **2** under (top) the zero field and (bottom) an applied d.c. field of 1.5 kOe.



**Supplementary Figure S4.** Variable-temperature, variable-frequency out-of-phase  $\chi''_M$  components of the a.c. magnetic susceptibility collected for a microcrystalline sample of **2** under different applied d.c. fields at 10 K.





**Supplementary Figure S5.** Variable temperature Cole-Cole plots for **2** in the zero field (top) and in the d.c. field of 1.5 kOe (bottom). Fitted parameters are compiled in Supplementary Tables S3-4.

**Supplementary Table S1.** Energies and Boltzman populations at 300 K of ten lowest states according to CASSCF/NEVPT2 calculations for **2**.

<b>States</b>	<b>Energy, cm<sup>-1</sup></b>	<b>Boltzmann populations at 300 K</b>
1a	0	3.65E-01
1b	0	3.65E-01
2a	220.6578	1.27E-01
2b	220.6578	1.27E-01
3a	840.5641	6.48E-03
3b	840.5641	6.48E-03
4a	1131.7264	1.60E-03
4b	1131.7264	1.60E-03
5a	6883.6942	1.68E-15
5b	6883.6942	1.68E-15

**Supplementary Table S2.** Fitted parameters to the Cole-Cole plots for **2** in the zero d.c. field as determined within the generalized Debye model ( $\tau$  – magnetic relaxation time,  $\alpha$  – distribution of relaxation times).

T(K)	$\alpha$	$\tau$ (s)
2	0.539	0.002864
3	0.515	0.002548
4	0.493	0.002373
5	0.463	0.002182
6	0.437	0.001994
7	0.403	0.001783
8	0.368	0.001568
9	0.332	0.001319
10	0.289	0.001146
11	0.251	0.000954
12	0.220	0.000773
13	0.193	0.000605
14	0.168	0.000462
15	0.135	0.000365
16	0.120	0.000250
17	0.092	0.000183
18	0.073	0.000114
19	0.076	0.000084
20	0.051	0.000065

**Supplementary Table S3.** Fitted parameters to the Cole-Cole plots for **2** in the d.c. field of 1.5 kOe as determined within the generalized Debye model ( $\tau$  – magnetic relaxation time,  $\alpha$  – distribution of relaxation times).

T(K)	$\alpha$	$\tau$ (s)
9	0.14469	0.01523
8	0.15451	0.0277
7	0.18099	0.05439
6	0.22103	0.12061
5	0.29178	0.33009
4	0.38005	1.26057
10	0.13231	0.00889
11	0.1225	0.00549
12	0.11974	0.0034
13	0.12065	0.00219
14	0.12138	0.00136
15	0.12571	8.47208E-4
16	0.13458	4.89689E-4
17	0.14518	2.70598E-4
18	0.1058	1.70023E-4

**Supplementary Table S4.** Parameters used to fit the Arrhenius plots from Figure 4 using approximations  $\tau = \tau_0 \exp(U_{eff}/kT)$  (linear in  $\ln(\tau)$  vs.  $1/T$  coordinates) and  $\tau^{-1} = AH^2T + \frac{B_1}{1+B_2H^2} + CT^n + \tau_0^{-1} \exp(-U/kT)$  (Eq.2). Parameters  $A$ ,  $B_1$  and  $B_2$  were fixed to values obtained by fitting field-dependent ac-magnetometry data (Fig. S4). As the applied magnetic field changes relative contributions of the individual relaxation pathways, the obtained values of  $\tau_0$  and  $B$  differ in the d.c. fields of 0 and 1.5 kOe.

	Zero d.c. field		1500 Oe d.c. field	
	linear approximation	approximation by Eq. 2	linear approximation	approximation by Eq. 2
$A, s^{-1}kOe^{-2}K^{-1}$	—	0.13	—	0.13
$B_1, s^{-1}$	—	490.7	—	490.7
$B_2, kOe^{-2}$	—	70	—	70
$C, s^{-1}K^{-5}$	—	0.002969	—	0.001017
$\tau_0, s$	$4.3 \cdot 10^{-7}$	$2.07 \cdot 10^{-9}$	$5.1 \cdot 10^{-8}$	$1.25 \cdot 10^{-9}$
$U, cm^{-1}$	71	152	101	152

## Supplementary references

- (43) Varzatskii, O. A.; Penkova, L. V.; Kats, S. V.; Dolganov, A. V.; Vologzhanina, A. V.; Pavlov, A. A.; Novikov, V. V.; Bogomyakov, A. S.; Nemykin, V. N.; Voloshin, Y. Z. *Inorg. Chem.* **2014**, 53, 3062.
- (44) Kahn, O. *Molecular magnetism*; VCH Publishers, Inc., 1993.
- (45) Neese, F. *Wiley Interdisciplinary Reviews-Computational Molecular Science* **2012**, 2, 73.
- (46) Perdew, J. P.; Burke, K.; Ernzerhof, M. *Phys. Rev. Lett.* **1996**, 77, 3865.
- (47) van Wüllen, C. *The Journal of Chemical Physics* **1998**, 109, 392.
- (48) Pantazis, D. A.; Chen, X.-Y.; Landis, C. R.; Neese, F. *Journal of Chemical Theory and Computation* **2008**, 4, 908.
- (49) Weigend, F.; Ahlrichs, R. *PCCP* **2005**, 7, 3297.
- (50) Klamt, A.; Schuurmann, G. *Journal of the Chemical Society-Perkin Transactions 2* **1993**, 799.
- (51) Adamo, C.; Barone, V. *J. Chem. Phys.* **1999**, 110, 6158.
- (52) Kaupp, M.; Bühl, M.; Malkin, V. G. *Calculation of NMR and EPR parameters: theory and applications*; John Wiley & Sons, 2006.
- (53) Atanasov, M.; Ganyushin, D.; Pantazis, D. A.; Sivalingam, K.; Neese, F. *Inorg. Chem.* **2011**, 50, 7460.